Radar Equivalent Snowpack: reducing the number of snow layers while retaining its microwave properties and bulk snow mass

Julien Meloche[1], Nicolas R. Leroux[2], Benoit Montpetit[1], Vincent Vionnet[2], and Chris Derksen[1]

[1]Climate Research Division, Environment and Climate Change Canada, Ontario, Canada

[2]Meteorological Research Division, Environment and Climate Change Canada, Quebec, Canada

Correspondence: Julien Meloche (julien.meloche@ec.gc.ca)

Abstract. Snow water equivalent (SWE) retrieval from Ku-band radar measurements is possible with complex retrieval algorithms involving prior information on the snowpack microstructure and a microwave radiative transfer model to link backscatter measurements to snow properties. A key variable in a retrieval is the number of snow layers, with more complex layering yielding richer information but at increased computational cost and number of unknowns. Here, we show the capabilities of a new method to simplify a complex multilayered snowpack to 2-3 layers, while nearly preserving the microwave scattering behavior of the snowpack and conserving the bulk snow water equivalent. This method, called Radar Equivalent Snowpack, is based on a K-means clustering algorithm to group the snow layers based on the extinction coefficient and a weighted average using the optical thickness applied to the snow properties. We evaluated our method using snow properties from simulations of the SVS-2/Crocus physical snow model at 11 sites spanning a large variety of climates across the world and the Snow Microwave Radiative Transfer model to calculate backscatter at 17.25 GHz. The layer simplification is done as an intermediate step between the physical modeling (SVS2/Crocus) and the microwave radiative transfer (SMRT). Grouping and averaging snow stratigraphy into 3 layers effectively reproduced the total snowpack backscatter of multi-layered snowpacks with overall root mean squared error = 0.5 dB and R^2 = 0.98. Using this methodology in SWE retrieval applications, this method can be used to simplify snowpacks and reduce the number of variables to optimize, while maintaining similar scattering behavior without compromising the modeled snowpack properties. Reduction in the mathematical complexity of SWE retrieval cost functions and reduction in computation of up to 80% can be gained by using fewer layers in the SWE retrieval.

1 Introduction

Snow Water Equivalent (SWE) is a key element of the hydrological cycle and an important component of the surface energy balance, so it must be well-represented in environmental prediction systems. Because conventional SWE observations are exceptionally sparse, new spaceborne radar missions to deliver SWE information are under development, such as the Canadian Terrestrial Snow Mass Mission (TSMM, Derksen et al., 2021; Tsang et al., 2022). A state-of-the-art SWE retrieval from the Ku-band radar measurements delivered by a mission like TSMM requires a radiative transfer model (RTM) to link snow properties to backscatter (Saberi et al., 2021; Zhu et al., 2021; Pan et al., 2017, 2023). Snow properties, including layer thickness, density, temperature, and microstructure (e.g., specific surface area), are necessary to properly model the microwave signal with an RTM. Prior, or *first-guess* information on layered snow properties is needed to constrain retrievals (Merkouriadi et al., 2021; Durand et al., 2024). This information can come from vertical snowpack measurements, either manually or using an instrument like a high-resolution snow penetrometer (SMP, Proksch et al., 2015). More typically, observations are unavailable, so snowpack information can come from physical snow models that provide multi-layered snow properties based on meteorological forcing data.

Detailed physical snow models like Crocus (Vionnet et al., 2012) and SNOWPACK (Bartelt and Lehning, 2002; Lehning et al., 2002) are one-dimensional multi-layer physical schemes that can model the evolution of the snowpack (including its microstructure) by taking into account energy exchange between the snow, the atmosphere, and the soil based on meteorological inputs. In Crocus, the snowpack is vertically discretized on a finite element grid with specific rules to allow the snowpack layering to evolve dynamically from new precipitation, compaction and/or metamorphism. One such rule is the dynamic attribution of the number of layers and thicknesses to simulate the snowpack layering. The minimum number is 3 layers but the maximum is 50 (Vionnet et al., 2012). Numerical snow models that use large numbers of layers can improve the representation of the dynamic physical processes within the snowpack, such as heat and mass fluxes, resulting in a better representation of the temperature profile. A better simulation of the vertical temperature profile within the snow improves the simulation of microstructure evolution and spring snowmelt initiation (Cristea et al., 2022). Therefore, there is a benefit to adding layers in physical modeling to improve the full vertical profile of snow properties.

Some algorithms couple a physical snow model and a snow RTM to retrieve SWE using microwave remote sensing data (Langlois et al., 2012; Larue et al., 2018; Singh et al., 2024). Snow RTMs can model the radar backscatter using snow parameters from complex layered snowpacks. In a SWE retrieval like Pan et al. (2017), the SWE (function of depth and density) of the different layers is estimated by minimizing the difference between the modeled and measured backscatter. To simulate the backscatter, most RTMs solve the radiative transfer equation based on the discrete ordinate and eigenvalue method (Picard et al., 2004), which discretizes the radiative transfer equation and solves a nonhomogeneous system of linear equations based on the number of layers. Increasing the number of snow layers thus increases the computational cost at many levels within the retrieval algorithm. Also, a larger numbers of layers increase the complexity of the retrieval by increasing the number of variables in the cost function. This is why current retrievals typically use a two-layer model (Saberi et al., 2021; Pan et al., 2017). Completely neglecting stratigraphy by using a one-layer model can affect the performance of the retrieval (Durand et al., 2011) because layering strongly influences the backscattering properties of snow (Rutter et al., 2016). A one-layer model oversimplifies the scattering behavior of the snowpack and so is not adequate in most cases (Rutter et al., 2019; Meloche et al., 2024; Montpetit et al., 2024). For this reason, a two or three-layer model provides notably better SWE retrievals by accounting for stratigraphy in a certain way (Pan et al., 2017; Saberi et al., 2021). In the end, there is a disconnect between needing several layers in a physical model to simulate a realistic microstructure profile but needing only 2 or 3 layers in SWE retrievals for computation simplicity.

To reduce the number of layers, a mass or thickness weighted average is commonly used to average all properties of the snowpack (Durand et al., 2011) and conserve snow mass (i.e., SWE). Singh et al. (2024) applied the same logic in averaging a multi-layered snowpack into a two-layered snowpack, and chose the height that corresponded to the maximum change in density to split the snowpack into two layers. Other SWE retrievals (Saberi et al., 2021) focused on arctic snowpack by setting the initial two-layer snowpack from well-documented layer properties (e.g., wind slab and depth hoar for Arctic snowpacks) (Rutter et al., 2019; Vargel et al., 2020; Derksen et al., 2009, 2012). For assimilation of passive microwave data, Larue et al. (2018) used a detailed physical snow model (Crocus) coupled with an RTM with a limit of 15 layers as a compromise between accuracy and computation time. Yu et al. (2021) proposed an interesting method to estimate an effective 1-layer snowpack for passive microwave applications that calculates a SWE weighted average for the microstructure parameter and preserves the reflectivity of the air/snow and snow/ground interface from the multilayer snowpack. With this approach, the scattering properties are better preserved. To our knowledge, a robust method still does not exist to effectively reduce the number of layers of a given snowpack while minimizing changes in scattering properties. This would allow the accuracy of SWE retrieval not to be compromised and the computation time to be reduced.

The goal of this paper is to develop a simple algorithm to convert a multi-layered snowpack with a large number of layers (20-50) into a simplified snowpack (2-3 layers) that preserves its snow mass and scattering behavior, thereby improving the computational cost with minimal impact on performance. The method should preserve backscatter within 1 dB, since it is the calibration uncertainty of most synthetic aperture radar (Schmidt et al., 2018). This study focuses only on evaluating our snowpack reduction method on dry snow in the context of SWE retrievals based on volume scattering. However, this method could potentially be used for wet snow since the extinction coefficient would be sensitive to liquid water via the absorption coefficient if the physical model correctly estimates the melt. To evaluate our method, we test it on multi-layered Crocus simulations at 11 sites across various snow climates over multiple seasons. From the 50-layer simulations (maximum layering), we compare various methods to obtain a "Radar Equivalent Snowpack" by evaluating differences in snow mass and simulated backscatter using the Snow Microwave Radiative Transfer Model (SMRT, Picard et al., 2018).

2 Methods

2.1 Study Site and Data

A total of 11 sites were selected to cover a wide range of snowpack conditions and climates, and meteorological forcing and evaluation datasets were previously published. Amongst the 11 sites, 6 are in mountain environments (Col de Porte, Kühtai and Weissfluhjoch in the European Alps, Reynolds Mountain, Senator Beck and Swamp Angel are in the Western USA); 2 are in tundra environments (Bylot and Trail Valley Creek in the Canadian high Arctic), 2 are in taiga environments (Umiujaq in the Canadian Boreal Forest and Sodankylä in the Finnish Boreal forest) and 1 is in a Maritime climate (Sapporo in Japan). Details of each dataset are shown in Table 1.

From the 11 sites, 3 were selected to more easily illustrate the methodology. These sites (TVC, WFJ and SAP) have distinct snowpack characteristics. The TVC arctic snowpack is characterized by a layer of highly scattering depth hoar with a dense wind slab on top. The WFJ alpine snowpack is characterized by a deep snowpack with progressive density increase from top to bottom with some melt-freeze crusts due to warming events throughout the season. The SAP snowpack is characterized by a similar alpine snowpack but more impacted by wet precipitation.

Table 1. Overview of sites used to evaluate Crocus snowpack layering reduction methods.

Site	Code	Source	Time Period	Lat. (°)	Lon. (°)	Elev. (m)	Country	Snow cover
Bylot	BYL	Domine et al. (2021)	2014-2019	73.15	-80.00	22	Canada	Arctic
Col de Porte	CDP	Menard and Essery (2019)	1994-2014	45.30	5.77	1325	France	Alpine
Kühtai	KUT	Krajči et al. (2017)	1990-2013	47.21	11.01	1920	Austria	Alpine
Reynolds Mountain	RME	Menard and Essery (2019)	1988-2008	43.19	-116.78	2060	USA	Alpine
Sapporo	SAP	Menard and Essery (2019)	2005-2015	43.08	141.34	15	Japan	Maritime
Senator Beck	SNB	Menard and Essery (2019)	2005-2015	37.91	-107.73	3714	USA	Alpine
Sodankylä	SOD	Menard and Essery (2019)	2007-2014	67.37	26.93	179	Finland	Taïga
Swamp Angel	SWA	Menard and Essery (2019)	2005-2015	37.91	-107.71	3371	USA	Alpine
Trail Valley Creek	TVC	Tutton et al. (2024)	2013-2018	68.75	-133.5	91	Canada	Arctic
Umiujaq	UMQ	Lackner et al. (2023)	2012-2020	56.56	-76.48	130	Canada	Taïga
Weissfluhjoch	WFJ	Menard and Essery (2019)	1996-2016	46.83	9.81	2536	Switzerland	Alpine

2.2 SVS2-CROCUS

The snowpack model Crocus (Brun et al., 1992; Lafaysse et al., 2017; Vionnet et al., 2012) was used to simulate the evolution of the snowpack properties, i.e. number of layers, and thickness, density, liquid water content, temperature, and specific surface area for each layer specifically. The version of Crocus used in this study is implemented into the Soil, Vegetation and Snow version 2 (SVS-2) land surface scheme (Garnaud et al., 2019; Vionnet et al., 2012; Woolley et al., 2024). The snowpack model is coupled to a multi-layered soil model that includes soil freezing and thawing (Boone et al., 2000). SVS-2 is an improvement to the SVS land surface scheme (Alavi et al., 2016; Husain et al., 2016; Leonardini et al., 2021) used at Environment and Climate Change Canada for hydrological prediction. For the simulations at the Arctic sites (Bylot and Trail Valley Creek), the Arctic version of Crocus (Royer et al., 2021b; Woolley et al., 2024) was used. This version improves the simulation of the wind slab properties and includes the impact of basal vegetation on the snowpack properties. This allows a better "arctic" density profile by increasing the wind slab density and lowering the depth hoar density.

At each site, simulations were run with a maximum number of 50 snow layers. Table B1 summarizes the options of Crocus for each physical process and the snow aging parameters (Gaillard et al., 2024) used for the simulations at the different sites. At the two arctic sites, the polar vegetation height was set to 10 cm (Woolley et al., 2024) and for taiga sites, it was set to 50 cm and 20 cm for the UMQ and SOD respectively. The model uses a time step of 10 minutes and the meteorological forcing is provided hourly.

2.3 Snow Microwave Radiative Transfer (SMRT)

SMRT is a multi-layer snow radiative transfer model that can compute backscatter in the microwave range. It considers each snow layer as a homogeneous random medium composed of air and ice and solves the radiative transfer equation for a multi-layered snowpack (Picard et al., 2018). Each snow layer is represented by temperature, density, thickness and microstructure parameters, all of which are provided by Crocus. One key component of SMRT is determining the scattering and absorption coefficients (κ_s, κ_a) of each layer. These coefficients dictate the radar scattering and absorbing behavior of the medium (snow). For snow, this generally implies that scattering (κ_s) dominates for dry snow, and absorption (κ_a) dominates for wet snow. The extinction coefficient ($\kappa_e = \kappa_s + \kappa_a$) characterizes the interaction within the medium by accounting for both coefficients and is a key parameter of the snow layer reduction algorithm presented in this paper. Multiple formulations of the coefficients can be used depending on the electromagnetic model, but here we focus on the Improved Born approximation (IBA, Mätzler, 1998) implemented in SMRT.

The phase function of snow in the 1-2 frame (e.g. ice particles (medium 2) in an air matrix (medium 1)) is defined by:

$$p_{\text{1-2 frame}}(\vartheta, \varphi) = \phi_\mathrm{i}(1-\phi_\mathrm{i})(\epsilon_2 - \epsilon_1)^2\, \mathrm{Y}^2(\epsilon_2, \epsilon_1) k_0^4\, M(|k_\mathrm{d}|) \sin^2\chi \tag{1}$$

where k_0 is the wavenumber in free space, ϕ_i is the volume fraction of the scattering constituent (ice) described $\phi_\mathrm{i} = \rho_\mathrm{snow}/\rho_\mathrm{ice}$ with ρ_snow the snow density (kg m^{-3}) and ρ_ice the pure ice density (kg m^{-3}), ϵ is the relative permittivity of both media and χ is the polarisation angle define from $\sin^2\chi = 1 - \sin^2\vartheta\cos^2\varphi$ for the scattering (ϑ) and the incident (φ) direction. The mean square field ratio (Y^2) accounts for the difference in the electric field between the background and scattering medium (see Picard et al. (2018) for equations). The microstructure term ($M(|k_\mathrm{d}|)$) is defined by the Fourier transform of the correlation function of the medium (ACF). Here, we used the exponential model (Mätzler, 2002)) where the ACF is characterized by a correlation length (l_mw) estimated by the specific surface area (SSA) and the snow density. More details on the ACF and $M(|k_\mathrm{d}|)$ can be found in Picard et al. (2018).The κ_s can be calculated from the following equation:

$$\kappa_s = \pi \int_0^\pi [\, p_{11}(\vartheta) + p_{22}(\vartheta)\,]\, d\vartheta \tag{2}$$

where $p_{11} = p_{\text{1-2 frame}}(\vartheta, \varphi = \pi/2)$ and $p_{22} = p_{\text{1-2 frame}}(\vartheta, \varphi = \pi)$ are defined from the phase function. The κ_a is defined by:

$$\kappa_a = 2k_0 \Im(\sqrt{\epsilon_\mathrm{eff}}) \tag{3}$$

where ϵ_eff is the effective permittivity using the Polden-van Santen general mixing formula (Sihvola, 1999).

In addition to the simulations using the full number of Crocus snow layers, SMRT was also used to simulate the backscatter of the snowpack to evaluate our averaging methods (Section 2.4). Crocus provides the layered snow density and SSA to estimate the microwave grain size with :

$$l_\mathrm{mw} = K l_\mathrm{p} = K\, \frac{4(1-\phi_\mathrm{i})}{\rho_\mathrm{ice}\, SSA} \tag{4}$$

where K is the polydispersity of the microstructure. The polydispersity was assumed to be 0.75 for all grain types in this experiment but future work could include a polydispersity for different Crocus-simulated grain types.

Simulations were performed first at the high Ku-band (17.25GHz), the TSMM frequency that is the most sensitive to volume scattering (Derksen et al., 2021) but later the frequency range, X to Ka-band, was also investigated. VV polarisation was the focus since HH will not be measured as part of TSMM (Derksen et al., 2021). A simple absorber for the background was used, i.e. no scattering from the ground is assumed, to only obtain the snow contribution to the modeled backscatter. The incident angle was set to 35 ° as a typical median value for SAR sensors such as TSMM. The snow layer interfaces were assumed to be flat.

2.4 Algorithm

The algorithm aims at reducing the number of snow layers to 2 or 3 relevant layers while preserving SWE and scattering behavior with respect to the reference snowpack (defined as the 50-layer Crocus simulations). The main goal is to develop a robust method to aggregate and average snow layer properties in a microwave SWE retrieval context. Figure 1 shows the general methodology to obtain a radar equivalent snowpack with reduced layers. The method is divided into two operations applied on layers : grouping and averaging.

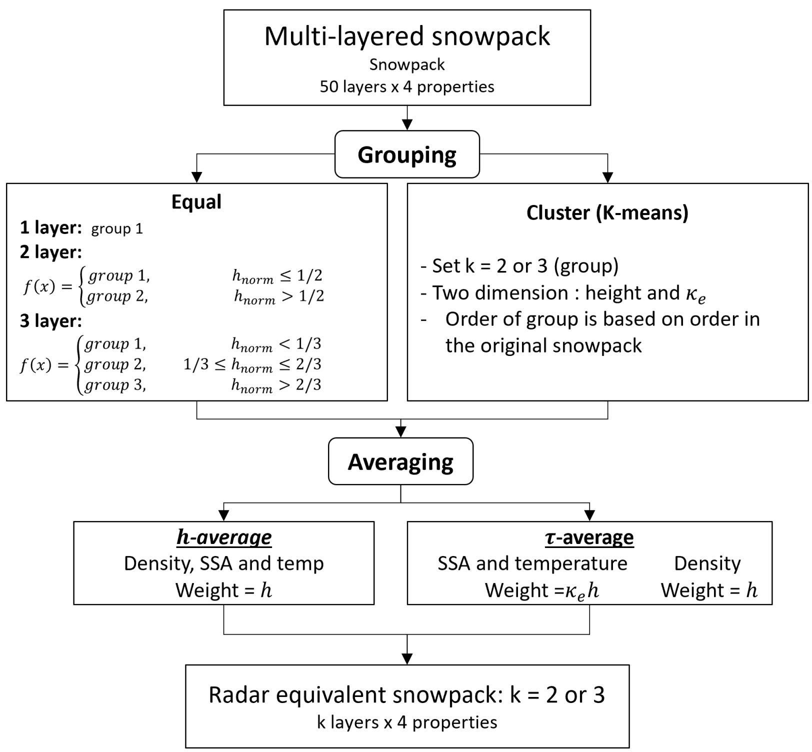

Figure 1. Schematic of the methodology. Necessary steps in the snowpack simplification are shown vertically and the different options (grouping and averaging) are shown horizontally where h_{norm} is the normalized height and h is the layer thickness. The 4 snow properties considered are: thickness, density, temperature and SSA.

The grouping of layers was done in two ways. The first method was used as a baseline comparison. This method (referred to as equal) aggregated layers based on the normalized height h_{norm}, which is the height of a layer divided by the thickness of the whole snowpack. For instance, if a snowpack is simplified into two layers, the top half of the snowpack, i.e all the layers with a height greater than 1/2 of the snowpack thickness would be aggregated into a first layer and the bottom half would contain all the layers with a height that are less than or equal to 1/2 of the snowpack thickness. This method is a basic way to obtain an equivalent snowpack with layers of equal thickness. Also, a 1-layer simplified snowpack was created by grouping all layers into 1 group to evaluate the worst-case scenario in reducing the number of layers. The second method, which is part of our proposed new methodology, was based on K-means clustering (Ikotun et al., 2023). This algorithm identifies groups within the parameter space by minimizing the variance within each group or cluster. First, it randomly initializes centroids for each group in the parameter space and then assigns each point to the initial groups based on the Euclidean distance to the nearest centroid. The centroids are updated to the mean position of all points within each group. The process is repeated iteratively until a convergence is reached (when the centroid positions no longer change significantly) or a fixed number of iterations is completed. A known issue with K-means is that the random initialization of the centroids can lead to non-representative clusters due to a local minimum reached in the convergence. To avoid this issue, the K-means++ initialization (Arthur and Vassilvitskii, 2007) was used, which ensures a smart initial choice of the centroids based on the empirical distance distribution of the points, essentially selecting centroids that are the furthest from each other. This speeds up the convergence and improves the quality of the clusters. In our case, the parameter space is the extinction coefficient κ_e of each layer and the respective layer height in the snowpack. Layers with strong extinction coefficients (high κ_e) will have strong interaction with the incident wave. A layer with a low extinction coefficient will be practically transparent to the incident wave. This method creates groups of layers based on their microwave properties κ_e and their location in the snowpack.

Once the grouping of layers was done, the snowpack layer properties (density, temperature, and SSA) were averaged. We investigated two different ways of averaging: (1) a weighted average based on h as a baseline (referred to as the h-average), and (2) a new weighted average based on the optical thickness $\tau = \kappa_e h$ (Zhu et al., 2021) for SSA and temperature (referred to as the τ-average). The h-average is used for density in both average methods, as it ensures the conservation of SWE. The average density of a snowpack with multiple layers of thickness h can be defined by:

$$\bar{\rho} = \frac{\sum_{\mathrm{i}=1}^{n} h_\mathrm{i}\rho_\mathrm{i}}{\sum_{\mathrm{i}=1}^{n} h_\mathrm{i}} \tag{5}$$

If we replace $\sum_{\mathrm{i}=1}^{n} h_\mathrm{i}$ by the thickness of the whole snowpack h_snow and rearrange equation 5, the SWE equation is obtained:

$$\mathrm{SWE} = \sum_{\mathrm{i}=1}^{n} h_\mathrm{i}\rho_\mathrm{i} = h_\mathrm{snow}\bar{\rho} \tag{6}$$

Finally, the thickness of each group is calculated by adding all the individual layer thicknesses within that group.

The backscatter was estimated for the reference simulation (maximum of layering from SVS2) and 5 other grouping methods referred to as 1-layer, 2-equal and 3-equal with the equal thickness layering method and 2-cluster and 3-cluster layers using the K-means cluster grouping. Both averaging methods were tested on the equal and cluster grouping to compare performance each method. The root mean squared error (RMSE) with the reference simulation is used to evaluate each method.

It is known that the backscatter in snow comes from both volume scattering and reflection at these interfaces. although interface reflection is small with respect to volume (except at nadir). When reducing the number of layers from 50 to 2, 48 interfaces are removed from the simulations. Although interface reflection is small with respect to volume, this reduces the overall internal layer reflections of the signal in the snowpack because of the reflected signal at each interface. However, if the permittivity contrast between two layers is low, then the reflection will be negligible. To quantify the effect of the reflections at each snow layer interface, backscatter simulations using transparent internal layers were used to estimate the influence of all the interfaces in the multi-layered snowpack configurations. The experiment referred to as transparent was done by leaving the surface to the default SMRT interface (flat Fresnel) and changing all internal interfaces to transparent, which yields no reflection and full transmission of the radar signal at each interface. This means setting transmission to 1 and reflection to 0. The snow-ground interface was not modified. The difference in backscatter was estimated between the reference simulation and the transparent simulation to estimate how much the internal interfaces are contributing to the total backscatter.

3 Results and Discussions

3.1 Grouping and averaging methods

Figure 2 presents examples of the 2-layer equivalent snowpacks (first column) and 3-layer equivalent snowpacks (second column) derived from the two methods (equal and cluster) for two different dates at WFJ. The equal method is shown by the dashed lines and the cluster method is shown by the colored symbols. The K-means method groups together layers with similar extinction, whereas the equal thickness method creates transitions that are not always consistent with transitions in scattering. For some vertical snow profiles, transitions between equal thickness layers can coincidentally occur with a change in κ_e (for example in Figure 2) but the K-means consistently identifies changes in κ_e. One particular case of cluster grouping is seen in Figure 2f, where the classification of certain layers is mixed (groups 1 and 2). The two layers classified as group 2 at approximately 50 cm depth were "added" to the bottom layer. The effect of this particular grouping is discussed later in the section.

The grouping and averaging methods were investigated first at three different sites that represent alpine (WFJ), maritime (SAP) and arctic (TVC) snowpacks. Figure 3 shows the simulated backscatter with SMRT for the 2013-2014 winter season. For easier representation, only the grouping with 3 layers is shown here. The 3-equal with h-average method was the worst in terms of reproducing the n-layer backscatter. The 3-cluster with h-average increases the performance but still cannot consistently replicate the n-layer backscatter across the whole season. The 3-equal with τ-average achieved similar performance to the 3-cluster with τ-average model, but had issues early in the season for WFJ and SAP. Using the τ-average was superior to the h-average to preserve the backscatter. The backscatter of the arctic snowpack at TVC is well represented for most grouping methods. Using the cluster method is not always better than equal grouping during the season. For some dates, the cluster falls closely to the equal grouping (Figure 2) and the resulting backscatter is similar.

To better understand the performance of the cluster approach, Figure 4 shows biases for the 3-equal and 3-cluster with h-average method as a function of snow properties. The 3-equal with h-average method shows increased negative biases for low density, and high SSA at the WFJ and SAP sites compared to biases for the cluster method that were smaller and constant across density and SSA. These layers have less scattering and low SWE (high SSA and low density) than other snow layers, supporting the idea that those snow layers were better handled by the cluster grouping because of the ability to identify and

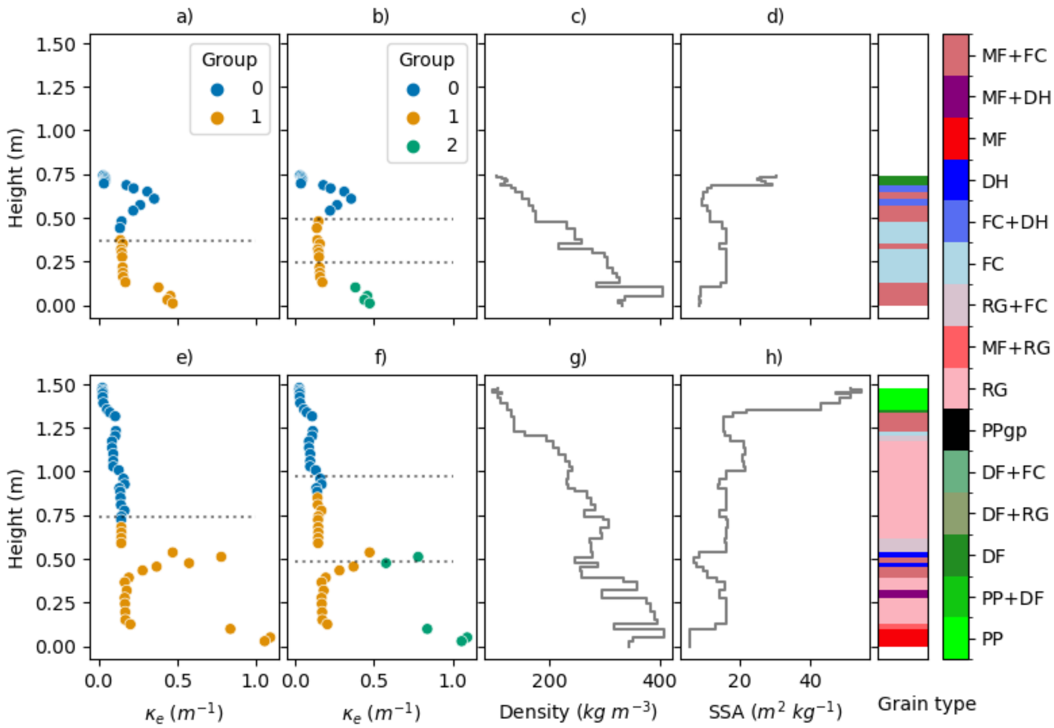

Figure 2. Snowpack properties (scattering, density, SSA and grain type) from Crocus and SMRT simulations at WFJ for the winter 2013-2014. The first row is 2013-12-08 and the second row is 2014-02-09. The grouping using the K-means cluster is shown by the colors in (a,b,e,f). The h_{norm} used for equal thickness grouping is also shown by the dashed lines. The colors and nomenclature for the grain types follow the international classification for seasonal snow on the ground (Fierz et al., 2009).

group these transparent layers. Biases for both methods tend to increase as the snow layers are warmer. For TVC, biases remain relatively small (< 1 dB) for the majority of the season because the SWE is fairly small (< 100 mm), and changes in stratigraphy are less frequent due to the lack of precipitation. Arctic snowpacks also tend to have a simple stratigraphy, well represented by a 2-layer snowpack (Vargel et al., 2020; Royer et al., 2021a).

Analysis of all sites and seasons (Table 2) produces results consistent with the example cases shown in Figure 3. Not surprisingly, aggregating the layers into a 1-layer snowpack with the h-average method resulted in the highest overall bias. Increasing the number of layers (from 1 to 3) as well as using a cluster grouping resulted in lower RMSE and greater R^2 (Table 2). Again, the 3-cluster with τ-average method is the most promising method to preserve SWE and the scattering behavior because the RMSE for all sites is the lowest (RMSE = 0.5 dB and R^2 = 0.98). TVC, KUT and SWA had the highest RMSE (0.7-0.8 dB) compared to BYL, CDP and UMQ, which had the lowest RMSE (0.3-0.4 dB). There is no pattern with respect to snow climate (alpine and arctic) and the performance of the 3-cluster with τ-average method. The 2-cluster with τ-average and 3-equal with τ-average method produced the second-best overall RMSE of 0.7 dB and R^2 = 0.97. The 3-equal with τ-average

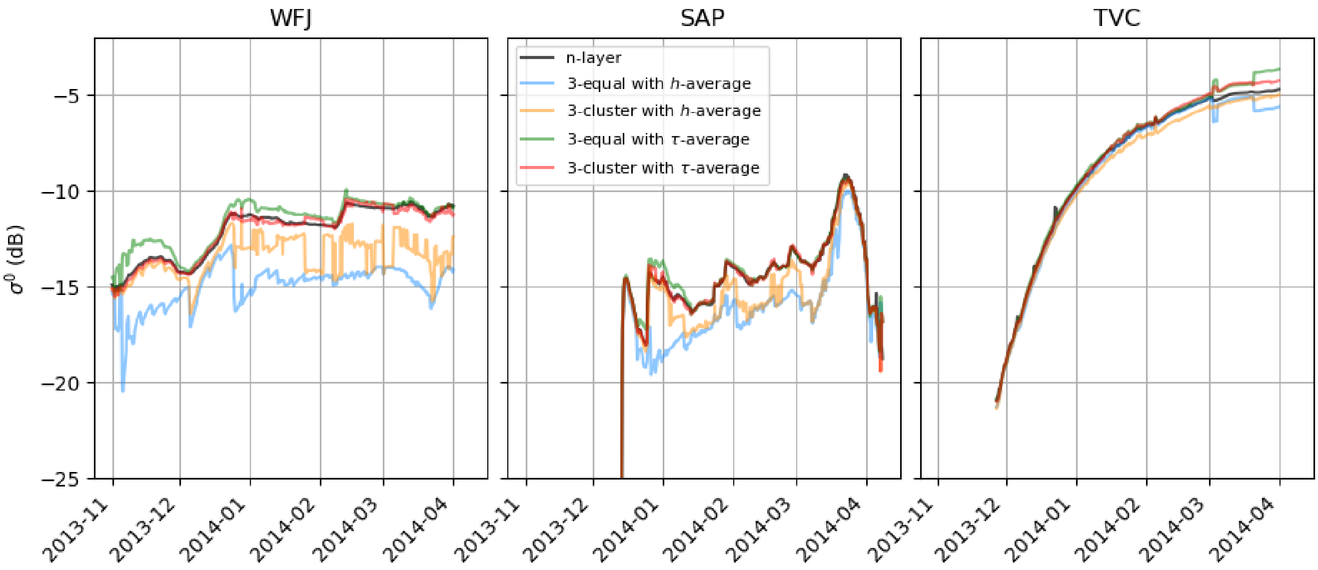

Figure 3. Backscatter time series for reference simulations and different 3-layer grouping and averaging methods. The simulations for the 2013-2014 season at WFJ, SAP and TVC are shown.

achieved lesser but similar performance to the 3-cluster with τ-average model. This indicates that the cluster grouping is less important in terms of preserving the microwave behavior than the τ-average of the snow properties.

Table 2. Overview of the RMSE and correlation coefficient (R^2) of the estimated backscatter for the different grouping and averaging methods for all sites and all seasons.

	Backscatter RMSE (dB), R^2							
Site	1-layer h-average	2-equal h-average	2-cluster τ-average	3-equal h-average	3-equal τ-average	3-cluster h-average	3-cluster τ-average	transparent
BYL	7.6, 0.39	1.8, 0.96	0.7, 0.99	1.4, 0.97	0.6, 0.99	0.6, 0.99	**0.4, 0.99**	0.4, 0.99
CDP	6.2, 0.64	3.5, 0.84	0.7, 0.99	2.5, 0.90	0.8, 0.98	0.7, 0.98	**0.5, 0.99**	0.3, 0.99
KUT	5.0, 0.65	2.5, 0.86	0.9, 0.96	1.9, 0.91	0.8, 0.97	1.1, 0.95	**0.7, 0.97**	0.3, 0.99
RME	4.7, 0.75	2.9, 0.87	0.7, 0.98	2.2, 0.91	0.7, 0.98	1.2, 0.96	**0.5, 0.99**	0.3, 0.99
SAP	4.4, 0.72	2.4, 0.88	0.4, 0.98	1.9, 0.91	0.5, 0.98	0.7, 0.98	**0.3, 0.99**	0.3, 0.99
SNB	2.7, 0.79	1.9, 0.89	0.7, 0.96	1.7, 0.92	0.6, 0.98	1.4, 0.93	**0.5, 0.98**	0.2, 0.99
SOD	5.5, 0.55	2.0, 0.91	0.6, 0.99	1.4, 0.95	0.6, 0.99	0.6, 0.99	**0.4, 0.99**	0.3, 0.99
SWA	4.1, 0.72	2.9, 0.80	0.9, 0.95	2.4, 0.84	0.7, 0.97	1.7, 0.90	**0.7, 0.97**	0.3, 0.99
TVC	9.0, 0.41	3.2, 0.71	0.9, 0.99	1.6, 0.91	0.7, 0.99	0.4, 0.99	**0.4, 0.99**	0.4, 0.99
UMQ	3.0, 0.78	2.0, 0.90	0.5, 0.99	1.7, 0.91	0.7, 0.98	0.7, 0.99	**0.3, 0.99**	0.2, 0.99
UFJ	4.0, 0.72	2.9, 0.84	0.9, 0.95	2.4, 0.88	0.7, 0.97	1.6, 0.92	**0.7, 0.97**	0.3, 0.99
All	5.1, 0.65	2.5, 0.86	0.7 , 0.97	1.9, 0.91	0.7, 0.98	1.0, 0.96	**0.5, 0.99**	0.3, 0.99

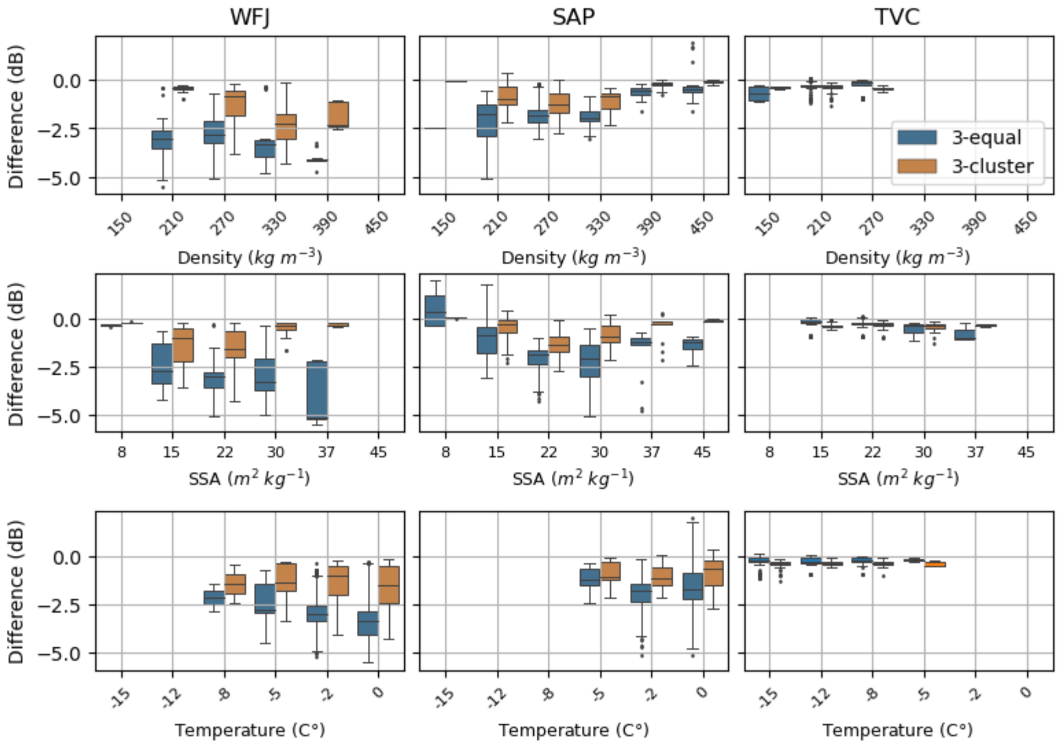

Figure 4. Box plot of difference in backscatter as a function of mean density, SSA and temperature per simulation for the sites WFJ, SAP and TVC for the 2013-2014 season.

Averaging layers using the h-average does not sufficiently reduce the backscatter RMSE below 1 dB. However, using τ-average brings the RMSE down to under 1 dB. The τ-average method was effective in preserving the backscatter because this averaging approach puts more weight on strong scattering layers due to κ_e. The thickness is also a good indicator of scattering because a thicker layer will scatter more than a thin layer with the same scattering properties. This is an effective way to average snow properties and preserve the scattering behavior of the snowpack. The τ-average method seems the most promising method to preserve the scattering behavior.

Transparent layer simulations yielded on average an RMSE of 0.3 dB from full layering simulations (Table 2). This indicates that on average the internal layering contributions are around 0.3 dB based on the number of layers from SVS2-Crocus simulations and the different sites and seasons. For the arctic sites (BYL, TVC and UMQ), the RMSE from the 3-cluster with τ-average method and the transparent experiment is the same, indicating that the snowpack reduction method is almost perfectly preserving the scattering of the snowpack with the exception of the layer contributions. For the other sites, especially alpine sites (KUT, SWA and UFJ), the RMSE of 0.7 dB for the 3-cluster with τ-average method is larger than the layering contribution, indicating there are still some effects from the reduction method that are not accounted for.

The issue raised in Figure 2 about mixed layers between groups can be further discussed with the results of the transparent layering. The two layers at 50 cm in Figure 2f that were grouped with the layers at the bottom with 3-Kmeans do not affect the scattering effect of the snowpack since they will be accounted for in the τ-average whether they are in group 0 or 1. However, attenuation of the scattering from these layers can differ if the layers are moved upward or downward in the snowpack. The other effect was the vertical change in permittivity that was modified, impacting the reflection of the signal on the internal layers. However, because the reflection of the internal layers was minimal ($\approx$ 0.3 dB) and change in backscatter was < 1 dB for all sites, it was concluded that the overall effect of this special grouping case was minimal.

The simulations were performed earlier at VV polarisation since it will be the primary polarisation of TSMM but similar simulations were also done at HH-polarisation (not shown here) and yielded a higher RMSE of 0.1 dB to VV-polarisation.

3.2 Frequency dependence

An analysis of frequency dependence was conducted across the X- to Ka-band range (10 to 40 GHz), encompassing regimes where volume scattering is significant. This interval includes the frequency utilized in the present study (17.25 GHz), which corresponds to the upper frequency selected for the Terrestrial Snow Mass Mission (Derksen et al., 2021). The errors between simulations with full layering and the 3-cluster with τ-average were similar to the values reported in Table 2 from 10 GHz, up to 30 GHz. The performance of the 3-cluster with τ-average method is based on κ_e which is frequency dependent. This allows us to obtain similar results when frequency (and sensitivity to volume scattering) increases. Although differences can be noted between sites, our method preserved similar performances from 10 GHz to 30 GHz. Under the 10 GHz, a different simulation setup would be needed since the soil contribution will dominate. Above 40 Ghz, the 3 cluster with τ-average method became similar to the 3-equal with h-average because the backscatter comes from the snow surface as the frequency increases and the penetration depth decreases.

3.3 Implications for SWE retrievals

In SWE retrieval applications, the number of variables that need to be optimized plays a crucial role in determining the accuracy and efficiency of the retrieval process. One of the most significant advantages of adopting a Radar Equivalent Snowpack representation is its ability to reduce the number of optimized variables without substantial loss of information. Now, an important choice still has to be done on whether 2 or 3 layers is best. We saw that backscatters from a 2-layer snowpack are slightly degraded compared to using a 3-layer snowpack (Table 2). Despite this small degradation with simplifying into 2 layers, retrieval applications could still benefit in terms of computational efficiency and reduced solution space, which can be advantageous for operational or large-scale applications. However, simplifying into 3 layers would offer a better representation of snowpacks across all climates.

In a Bayesian retrieval, calculating the mismatch term involves running a radiative transfer model and then optimizing the resulting posterior parameters. Using the Radar Equivalent Snowpack would imply that the optimization is performed for a snowpack represented by a reduced number of layers, rather than its full complexity. Concurrently, the prior distributions for snow properties, which are sourced from SVS2, are also reduced to this number of layers. This consistent approach ensures

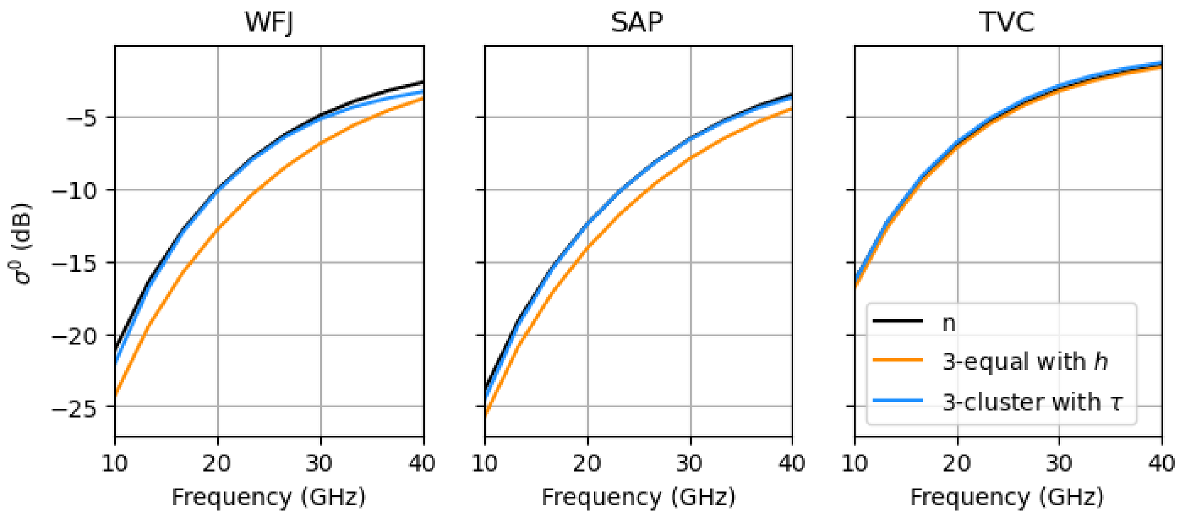

Figure 5. Backscatter simulations of 3-equal with h-average and 3-cluster with τ-average methods as a function of frequency

that both the forward modeling for the mismatch term and the prior information is based on a comparable, simplified structural representation of the snowpack.

4 Conclusions

In this paper, we showed the performance of our methods to simplify complex multilayered snowpacks to less than or equal to 3 layers while preserving their microwave scattering behavior and bulk snow mass. We evaluated our method using simulated snow properties generated by the Crocus snowpack scheme at 11 sites which were input to the SMRT model to calculate backscatter at 17.25 GHz and VV polarization. This emulates potential future measurements from the Canadian Terrestrial Snow Mass Mission. The method was a K-means clustering algorithm that groups the snow layers based on the extinction coefficient and the height of the layer in the snowpack. Then, a weighted average using the extinction coefficient and the thickness was applied to the snow properties, except for density, for which snow layer thickness was used as a weight to conserve SWE. We found that the averaging method was more important than the grouping method to preserve the backscatter. Reducing the original 50 snow layers into 3 layers using this method reproduced the snowpack backscatter of the original multi-layered snowpacks with an overall RMSE = 0.5 dB and R^2 = 0.98. Using this methodology in SWE retrieval algorithms allows snowpack simplification without nearly impacting the scattering behavior or compromising the geophysical properties. Reduction in mathematical complexity of SWE cost function and reduction in computation up to 80% (appendix A1) can be gained by using fewer layers in SWE retrievals.

We proposed the Radar Equivalent Snowpack, a simple method that can also be applied to other fields of study that need to simplify a multilayered snowpack without compromising the electromagnetic properties of snow. The algorithm averages snow layers to obtain effective layers with snow properties that have an electromagnetic equivalent, so the potential application must be specific to the chosen frequency. This method could be adapted to passive microwave remote sensing where the signal is also highly dependent on snow scattering, including ice sheet or sea ice remote sensing where the microwave signal could be simplified to focus on radiative relevant layers. For the TSMM workflow, this Radar Equivalent Snowpack allows for simplifying the modeled snowpack from the SVS2-Crocus and reducing the number of unknown in the SWE retrieval. It can also be used in assimilation schemes to reduce the computational time required to calculate a backscatter ensemble from a collection of snowpack members. For these reasons, this method offers an effective way to link physical snow modeling and snow radiative transfer modeling together in SWE retrievals.

Code and data availability. Code are Available on at https://github.com/JulienMeloche/radar_equivalent_snowpack

Author contributions. JM, NL and BM wrote the manuscript with contributions from all co-authors. All co-authors designed the experiment. JM and NL performed the analysis. VV and NL developped SVS-2. All co-authors reviewed the manuscript and provided analysis guidance.

Competing interests. Some authors are members of the editorial board of The Cryosphere.

Acknowledgements. The study was supported by Environment and Climate Change Canada and made possible by open source developpement of the SMRT and Crocus model.

Appendix A

A1 Computation efficiency

Computation time was also estimated for each method to evaluate the gain in computational efficiency. The reduction in computation time of the backscatter for reducing a complex multilayered snowpack (50 to 10 layers) to 2 or 3 layers is shown in Table A1. The largest reduction in computation time was from 50 layers to 2 layers with 87% and the smallest was from 10 to 3 layers with 39%. Even the smallest reduction is considerable and motivates this work in the context of operational SWE retrieval implementations, where these computations have to be done at large scales.

Appendix B

Table A1. Computation time of backscatter with SMRT and grouping methods. Results in various configurations of the number of layers are shown here. The grouping times for the Kmeans method are also shown. The backscatter computation time for 3 layer is 0.15 s and 0.12 for 2 layers. The grouping and averaging (3-cluster with τ-average) method takes 0.005 s.

		Reduction (%)	
Number of layers	**Computation time (s)**	**to 3 layers**	**to 2 layers**
50 layers	0.90	83	87
40 layers	0.80	81	85
30 layers	0.67	78	82
20 layers	0.46	68	75
10 layers	0.25	39	53

Table B1. Crocus schemes and parameters used at the different sites. The meaning of the Crocus schemes can be found in Lafaysse et al. (2017) and Woolley et al. (2024). The different options are defined in their respective paper; B21: modified C13 from Carmagnola et al. (2014), B92: Brun et al. (1992), R21: Royer et al. (2021b), V12: Vionnet et al. (2012) and Y81: Yen (1981). The γ parameter represents the snow ageing coefficient and was determined at the sites in (Gaillard et al., 2024), except for Reynolds Mountain for which the default value of 60 days was used.

Site	**Metamorphism**	**Radiation**	**Snowfall density**	**Thermal conductivity**	**Water percolation**	**Compaction**	γ **(d)**
Bylot	B21	B92	R21	Y81	B92	R21	900
Col de Porte	B21	B92	V12	Y81	B92	B92	20
Kühtai	B21	B92	V12	Y81	B92	B92	10
Reynolds Mountain	B21	B92	V12	Y81	B92	B92	60
Sapporo	B21	B92	V12	Y81	B92	B92	40
Senator Beck	B21	B92	V12	Y81	B92	B92	60
Sodankylä	B21	B92	R21	Y81	B92	R21	150
Swamp Angel	B21	B92	V12	Y81	B92	B92	60
Trail Valley Creek	B21	B92	R21	Y81	B92	R21	900
Umiujaq	B21	B92	R21	Y81	B92	R21	200
Weissfluhjoch	B21	B92	V12	Y81	B92	B92	200

References

Alavi, N., Bélair, S., Fortin, V., Zhang, S., Husain, S. Z., Carrera, M. L., and Abrahamowicz, M.: Warm Season Evaluation of Soil Moisture Prediction in the Soil, Vegetation, and Snow (SVS) Scheme, Journal of Hydrometeorology, 17, 2315–2332, https://doi.org/10.1175/JHM-D-15-0189.1, 2016.

Arthur, D. and Vassilvitskii, S.: K-Means++: The Advantages of Careful Seeding, Society for Industrial and Applied Mathematics, pp. 1027–1035, 2007.

Bartelt, P. and Lehning, M.: A Physical SNOWPACK Model for the Swiss Avalanche Warning, Cold Regions Science and Technology, 35, 123–145, https://doi.org/10.1016/S0165-232X(02)00074-5, 2002.

Boone, A., Masson, V., Meyers, T., and Noilhan, J.: The Influence of the Inclusion of Soil Freezing on Simulations by a Soil–Vegetation–Atmosphere Transfer Scheme, Journal of Applied Meteorology, 39, 1544–1569, https://doi.org/10.1175/1520-0450(2000)039<1544:TIOTIO>2.0.CO;2, 2000.

Brun, E., David, P., Sudul, M., and Brunot, G.: A Numerical Model to Simulate Snow-Cover Stratigraphy for Operational Avalanche Forecasting, Journal of Glaciology, 38, 13–22, https://doi.org/10.3189/S0022143000009552, 1992.

Carmagnola, C. M., Morin, S., Lafaysse, M., Domine, F., Lesaffre, B., Lejeune, Y., Picard, G., and Arnaud, L.: Implementation and Evaluation of Prognostic Representations of the Optical Diameter of Snow in the SURFEX/ISBA-Crocus Detailed Snowpack Model, The Cryosphere, 2014.

Cristea, N. C., Bennett, A., Nijssen, B., and Lundquist, J. D.: When and Where Are Multiple Snow Layers Important for Simulations of Snow Accumulation and Melt?, Water Resources Research, 58, e2020WR028 993, https://doi.org/10.1029/2020WR028993, 2022.

Derksen, C., Silis, A., Sturm, M., Holmgren, J., Liston, G. E., Huntington, H., and Solie, D.: Northwest Territories and Nunavut Snow Characteristics from a Subarctic Traverse: Implications for Passive Microwave Remote Sensing, Journal of Hydrometeorology, 10, 448–463, https://doi.org/10.1175/2008JHM1074.1, 2009.

Derksen, C., Toose, P., Lemmetyinen, J., Pulliainen, J., Langlois, A., Rutter, N., and Fuller, M.: Evaluation of Passive Microwave Brightness Temperature Simulations and Snow Water Equivalent Retrievals through a Winter Season, Remote Sensing of Environment, 117, 236–248, https://doi.org/10.1016/j.rse.2011.09.021, 2012.

Derksen, C., King, J., Belair, S., Garnaud, C., Vionnet, V., Fortin, V., Lemmetyinen, J., Crevier, Y., Plourde, P., Lawrence, B., van Mierlo, H., Burbidge, G., and Siqueira, P.: Development of the Terrestrial Snow Mass Mission, in: 2021 IEEE International Geoscience and Remote Sensing Symposium IGARSS, pp. 614–617, IEEE, Brussels, Belgium, https://doi.org/10.1109/IGARSS47720.2021.9553496, 2021.

Domine, F., Lackner, G., Sarrazin, D., Poirier, M., and Belke-Brea, M.: Meteorological, Snow and Soil Data (2013–2019) from a Herb Tundra Permafrost Site at Bylot Island, Canadian High Arctic, for Driving and Testing Snow and Land Surface Models, Earth System Science Data, 13, 4331–4348, https://doi.org/10.5194/essd-13-4331-2021, 2021.

Durand, M., Kim, E. J., Margulis, S. A., and Molotch, N. P.: A First-Order Characterization of Errors From Neglecting Stratigraphy in Forward and Inverse Passive Microwave Modeling of Snow, IEEE Geoscience and Remote Sensing Letters, 8, 730–734, https://doi.org/10.1109/LGRS.2011.2105243, 2011.

Durand, M., Johnson, J. T., Dechow, J., Tsang, L., Borah, F., and Kim, E. J.: Retrieval of Snow Water Equivalent from Dual-Frequency Radar Measurements: Using Time Series to Overcome the Need for Accurate a Priori Information, The Cryosphere, 2024.

Fierz, C., Armstrong, R. L., Durand, Y., Etchevers, P., Greene, E., McClung, D. M., Nishimura, K., Satyawali, P., and Sokratov, S. A.: The International Classification for Seasonal Snow on the Ground, 1, 2009.

Gaillard, M., Vionnet, V., Lafaysse, M., Dumont, M., and Ginoux, P.: Improving Large-Scale Snow Albedo Modelling Using a Climatology of Light-Absorbing Particle Deposition, https://doi.org/10.5194/egusphere-2024-1795, 2024.

Garnaud, C., Bélair, S., Carrera, M. L., Derksen, C., Bilodeau, B., Abrahamowicz, M., Gauthier, N., and Vionnet, V.: Quantifying Snow Mass Mission Concept Trade-Offs Using an Observing System Simulation Experiment, Journal of Hydrometeorology, 20, 155–173, https://doi.org/10.1175/JHM-D-17-0241.1, 2019.

Husain, S. Z., Alavi, N., Bélair, S., Carrera, M., Zhang, S., Fortin, V., Abrahamowicz, M., and Gauthier, N.: The Multibudget Soil, Vegetation, and Snow (SVS) Scheme for Land Surface Parameterization: Offline Warm Season Evaluation, Journal of Hydrometeorology, 17, 2293–2313, https://doi.org/10.1175/JHM-D-15-0228.1, 2016.

Ikotun, A. M., Ezugwu, A. E., Abualigah, L., Abuhaija, B., and Heming, J.: K-Means Clustering Algorithms: A Comprehensive Review, Variants Analysis, and Advances in the Era of Big Data, Information Sciences, 622, 178–210, https://doi.org/10.1016/j.ins.2022.11.139, 2023.

Krajči, P., Kirnbauer, R., Parajka, J., Schöber, J., and Blöschl, G.: The Kühtai Data Set: 25 Years of Lysimetric, Snow Pillow, and Meteorological Measurements, Water Resources Research, 53, 5158–5165, https://doi.org/10.1002/2017WR020445, 2017.

Lackner, G., Domine, F., Sarrazin, D., Nadeau, D., and Belke-Brea, M.: Meteorological, Snow and Soil Data, CO_2, Water and Energy Fluxes, from a Low-Arctic Valley in the Forest-Tundra Ecotone of Northern Quebec, Preprint, ESSD – Land/Energy and Emissions, https://doi.org/10.5194/essd-2023-7, 2023.

Lafaysse, M., Cluzet, B., Dumont, M., Lejeune, Y., Vionnet, V., and Morin, S.: A Multiphysical Ensemble System of Numerical Snow Modelling, The Cryosphere, 11, 1173–1198, https://doi.org/10.5194/tc-11-1173-2017, 2017.

Langlois, A., Royer, A., Derksen, C., Montpetit, B., Dupont, F., and Goïta, K.: Coupling the Snow Thermodynamic Model SNOWPACK with the Microwave Emission Model of Layered Snowpacks for Subarctic and Arctic Snow Water Equivalent Retrievals: SWE RETRIEVAL USING SNOW AND MICROWAVE MODELS, Water Resources Research, 48, https://doi.org/10.1029/2012WR012133, 2012.

Larue, F., Royer, A., De Sève, D., Roy, A., Picard, G., Vionnet, V., and Cosme, E.: Simulation and Assimilation of Passive Microwave Data Using a Snowpack Model Coupled to a Calibrated Radiative Transfer Model Over Northeastern Canada, Water Resources Research, 54, 4823–4848, https://doi.org/10.1029/2017WR022132, 2018.

Lehning, M., Bartelt, P., Brown, B., Fierz, C., and Satyawali, P.: A Physical SNOWPACK Model for the Swiss Avalanche Warning Part II. Snow Microstructure, Cold Regions Science and Technology, p. 21, 2002.

Leonardini, G., Anctil, F., Vionnet, V., Abrahamowicz, M., Nadeau, D. F., and Fortin, V.: Evaluation of the Snow Cover in the Soil, Vegetation, and Snow (SVS) Land Surface Model, Journal of Hydrometeorology, https://doi.org/10.1175/JHM-D-20-0249.1, 2021.

Mätzler, C.: Improved Born Approximation for Scattering of Radiation in a Granular Medium, Journal of Applied Physics, 83, 6111–6117, https://doi.org/10.1063/1.367496, 1998.

Mätzler, C.: Relation between Grain-Size and Correlation Length of Snow, Journal of Glaciology, 48, 461–466, https://doi.org/10.3189/172756502781831287, 2002.

Meloche, J., Royer, A., Roy, A., Langlois, A., and Picard, G.: Improvement of Polar Snow Microwave Brightness Temperature Simulations for Dense Wind Slab and Large Grain, IEEE Transactions on Geoscience and Remote Sensing, 62, 1–10, https://doi.org/10.1109/TGRS.2024.3428394, 2024.

Menard, C. and Essery, R.: ESM-SnowMIP Meteorological and Evaluation Datasets at Ten Reference Sites (in Situ and Bias Corrected Reanalysis Data), https://doi.org/10.1594/PANGAEA.897575, 2019.

Merkouriadi, I., Lemmetyinen, J., Liston, G. E., and Pulliainen, J.: Solving Challenges of Assimilating Microwave Remote Sensing Signatures With a Physical Model to Estimate Snow Water Equivalent, Water Resources Research, 57, https://doi.org/10.1029/2021WR030119, 2021.

Montpetit, B., King, J., Meloche, J., Derksen, C., Siqueira, P., Adam, J. M., Toose, P., Brady, M., Wendleder, A., Vionnet, V., and Leroux, N. R.: Retrieval of Snow and Soil Properties for Forward Radiative Transfer Modeling of Airborne Ku-band SAR to Estimate Snow Water

Equivalent: The Trail Valley Creek 2018/19 Snow Experiment, The Cryosphere, 18, 3857–3874, https://doi.org/10.5194/tc-18-3857-2024, 2024.

Pan, J., Durand, M. T., Vander Jagt, B. J., and Liu, D.: Application of a Markov Chain Monte Carlo Algorithm for Snow Water Equivalent Retrieval from Passive Microwave Measurements, Remote Sensing of Environment, 192, 150–165, https://doi.org/10.1016/j.rse.2017.02.006, 2017.

Pan, J., Durand, M., Lemmetyinen, J., Liu, D., and Shi, J.: Snow Water Equivalent Retrieved from X- and Dual Ku-band Scatterometer Measurements at Sodankylä Using the Markov Chain Monte Carlo Method, Preprint, Snow/Remote Sensing, https://doi.org/10.5194/tc-2023-85, 2023.

Picard, G., Le Toan, T., Quegan, S., Caraglio, Y., and Castel, T.: Radiative Transfer Modeling of Cross-Polarized Backscatter from a Pine Forest Using the Discrete Ordinate and Eigenvalue Method, IEEE Transactions on Geoscience and Remote Sensing, 42, 1720–1730, https://doi.org/10.1109/TGRS.2004.831229, 2004.

Picard, G., Sandells, M., and Löwe, H.: SMRT: An Active–Passive Microwave Radiative Transfer Model for Snow with Multiple Microstructure and Scattering Formulations (v1.0), Geoscientific Model Development, 11, 2763–2788, https://doi.org/10.5194/gmd-11-2763-2018, 2018.

Proksch, M., Löwe, H., and Schneebeli, M.: Density, Specific Surface Area, and Correlation Length of Snow Measured by High-Resolution Penetrometry, Journal of Geophysical Research: Earth Surface, 120, 346–362, https://doi.org/10.1002/2014JF003266, 2015.

Royer, A., Domine, F., Roy, A., Langlois, A., Marchand, N., and Davesne, G.: New Northern Snowpack Classification Linked to Vegetation Cover on a Latitudinal Mega-Transect across Northeastern Canada, Écoscience, 28, 225–242, https://doi.org/10.1080/11956860.2021.1898775, 2021a.

Royer, A., Picard, G., Vargel, C., Langlois, A., Gouttevin, I., and Dumont, M.: Improved Simulation of Arctic Circumpolar Land Area Snow Properties and Soil Temperatures, Frontiers in Earth Science, 9, 685 140, https://doi.org/10.3389/feart.2021.685140, 2021b.

Rutter, N., Marshall, H.-P., Tape, K., Essery, R., and King, J.: Impact of Spatial Averaging on Radar Reflectivity at Internal Snowpack Layer Boundaries, Journal of Glaciology, 62, 1065–1074, https://doi.org/10.1017/jog.2016.99, 2016.

Rutter, N., Sandells, M. J., Derksen, C., King, J., Toose, P., Wake, L., Watts, T., Essery, R., Roy, A., Royer, A., Marsh, P., Larsen, C., and Sturm, M.: Effect of Snow Microstructure Variability on Ku-band Radar Snow Water Equivalent Retrievals, The Cryosphere, 13, 3045–3059, https://doi.org/10.5194/tc-13-3045-2019, 2019.

Saberi, N., Kelly, R., Pan, J., Durand, M., Goh, J., and Scott, K. A.: The Use of a Monte Carlo Markov Chain Method for Snow-Depth Retrievals: A Case Study Based on Airborne Microwave Observations and Emission Modeling Experiments of Tundra Snow, IEEE Transactions on Geoscience and Remote Sensing, 59, 1876–1889, https://doi.org/10.1109/TGRS.2020.3004594, 2021.

Schmidt, K., Tous Ramon, N., and Schwerdt, M.: Radiometric Accuracy and Stability of Sentinel-1A Determined Using Point Targets, International Journal of Microwave and Wireless Technologies, 10, 538–546, https://doi.org/10.1017/S1759078718000016, 2018.

Sihvola, A.: Electromagnetic Mixing Formulas and Applications, 1999.

Singh, S., Durand, M., Kim, E., and Barros, A. P.: Bayesian Physical–Statistical Retrieval of Snow Water Equivalent and Snow Depth from X- and Ku-band Synthetic Aperture Radar – Demonstration Using Airborne SnowSAr in SnowEx'17, The Cryosphere, 18, 747–773, https://doi.org/10.5194/tc-18-747-2024, 2024.

Tsang, L., Durand, M., Derksen, C., Barros, A. P., Kang, D.-H., Lievens, H., Marshall, H.-P., Zhu, J., Johnson, J., King, J., Lemmetyinen, J., Sandells, M., Rutter, N., Siqueira, P., Nolin, A., Osmanoglu, B., Vuyovich, C., Kim, E., Taylor, D., Merkouriadi, I., Brucker, L., Navari, M., Dumont, M., Kelly, R., Kim, R. S., Liao, T.-H., Borah, F., and Xu, X.: Review Article: Global Monitoring of Snow Water Equivalent Using High-Frequency Radar Remote Sensing, The Cryosphere, 16, 3531–3573, https://doi.org/10.5194/tc-16-3531-2022, 2022.

Tutton, R., Darkin, B., Essery, R., Griffith, J., Gosselin, G., Marsh, P., Sonnentag, O., Thorne, R., and Walker, B.: A Hydro-Meterological Dataset from the Taiga-Tundra Ecotone in the Western Canadian Arctic: Trail Valley Creek, Northwest Territories (1991-2023), https://doi.org/10.5683/SP3/BXV4D, 2024.

Vargel, C., Royer, A., St-Jean-Rondeau, O., Picard, G., Roy, A., Sasseville, V., and Langlois, A.: Arctic and Subarctic Snow Microstructure Analysis for Microwave Brightness Temperature Simulations, Remote Sensing of Environment, 242, 111 754, https://doi.org/10.1016/j.rse.2020.111754, 2020.

Vionnet, V., Brun, E., Morin, S., Boone, A., Faroux, S., Le Moigne, P., Martin, E., and Willemet, J.-M.: The Detailed Snowpack Scheme Crocus and Its Implementation in SURFEX v7.2, Geoscientific Model Development, 5, 773–791, https://doi.org/10.5194/gmd-5-773-2012, 2012.

Woolley, G. J., Rutter, N., Wake, L., Vionnet, V., Derksen, C., Essery, R., Marsh, P., Tutton, R., Walker, B., Lafaysse, M., and Pritchard, D.: Multi-Physics Ensemble Modelling of Arctic Tundra Snowpack Properties, https://doi.org/10.5194/egusphere-2024-1237, 2024.

Yen, Y.-C.: Review of the Thermal Properties of Snow, Ice and Sea Ice, Tech. Rep. Cold Regions Research and Engineering Laboratory, 1981.

Yu, Y., Pan, J., and Shi, J.: Evaluation of the Effective Microstructure Parameter of the Microwave Emission Model of Layered Snowpack for Multiple-Layer Snow, Remote Sensing, 13, 2012, https://doi.org/10.3390/rs13102012, 2021.

Zhu, J., Tan, S., Tsang, L., Kang, D.-H., and Kim, E.: Snow Water Equivalent Retrieval Using Active and Passive Microwave Observations, Water Resources Research, 57, https://doi.org/10.1029/2020WR027563, 2021.